

RESEARCH ARTICLE

Open Access



# Chromophoric cerium oxide nanoparticle-loaded sucking disk-type strip sensor for optical measurement of glucose in tear fluid

Sijin Park<sup>1†</sup>, Dong Yeon Nam<sup>2†</sup>, Hee-Jae Jeon<sup>3†</sup>, Jae Hoon Han<sup>2†</sup>, Dawon Jang<sup>1</sup>, Juil Hwang<sup>4</sup>, Yeong-Seo Park<sup>3</sup>, Young-Geun Han<sup>4</sup>, Young Bin Choy<sup>2,5,6\*</sup> and Dong Yun Lee<sup>1,7,8\*</sup> 

## Abstract

**Background** Noninvasive monitoring of tear glucose levels can be convenient for patients to manage their diabetes mellitus. However, there are issues with monitoring tear glucose levels, such as the invasiveness of some methods, the miniaturization, inaccuracy, or the high cost of wearable devices. To overcome the issues, we newly designed a sucking disk-type (SD) strip biosensor that can quickly suck tear fluid and contains cerium oxide nanoparticle (CNP) that causes a unique color change according to the glucose level of the tear without complicated electronic components.

**Methods** The SD strip biosensor composed of three distinct parts (tip, channel, and reaction chamber) was designed to contain the sensing paper, onto which tear fluid can be collected and delivered. The sensing paper treated with CNP/APTS (aminopropyltriethoxysilane) /GOx (glucose oxidase) was characterized. Then we carried out the reliability of the SD strip biosensor in the diabetic rabbit animals. We quantitatively analyzed the color values of the SD strip biosensor through the colorimetric analysis algorithm.

**Results** We contacted the inferior palpebral conjunctiva (IPC) of a diabetic rabbit eye using an SD strip biosensor to collect tears without eye irritation and successfully verified the performance and quantitative efficacy of the sensor. An image processing algorithm that can optimize measurement accuracy is developed for accurate color change measurement of SD strip biosensors. The validation tests show a good correlation between glucose concentrations measured in the tear and blood.

**Conclusion** Our findings demonstrate that the CNP-embedded SD strip biosensor and the associated image processing can simply monitor tear glucose to manage diabetes mellitus.

**Keywords** Sucking disk-type (SD) strip biosensor, Cerium oxide nanoparticles (CNPs), Image processing algorithms, Tear glucose, Diabetes

<sup>†</sup>Sijin Park, Dong Yeon Nam, Hee-Jae Jeon and Jae Hoon Han contributed equally to this work.

\*Correspondence:

Young Bin Choy

ybchoy@snu.ac.kr

Dong Yun Lee

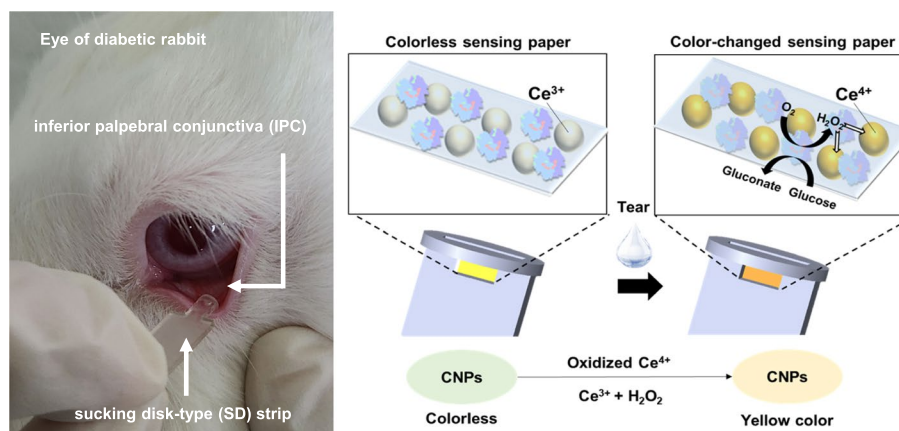
dongyunlee@hanyang.ac.kr

Full list of author information is available at the end of the article



© The Author(s) 2023. **Open Access** This article is licensed under a Creative Commons Attribution 4.0 International License, which permits use, sharing, adaptation, distribution and reproduction in any medium or format, as long as you give appropriate credit to the original author(s) and the source, provide a link to the Creative Commons licence, and indicate if changes were made. The images or other third party material in this article are included in the article's Creative Commons licence, unless indicated otherwise in a credit line to the material. If material is not included in the article's Creative Commons licence and your intended use is not permitted by statutory regulation or exceeds the permitted use, you will need to obtain permission directly from the copyright holder. To view a copy of this licence, visit <http://creativecommons.org/licenses/by/4.0/>. The Creative Commons Public Domain Dedication waiver (<http://creativecommons.org/publicdomain/zero/1.0/>) applies to the data made available in this article, unless otherwise stated in a credit line to the data.

## Graphical Abstract



## Background

Diabetes is a chronic disease that can lead to serious complications such as cardiovascular diseases, diabetic retinopathy, diabetic nephropathy, and diabetic neuropathy [1, 2]. Early diagnosis and proper blood glucose management are important to control and prevent the progression of the disease and its complications [3–8]. Conventional point-of-care glucose monitoring systems and blood glucose self-testing (BGST) are commonly used in diabetes management [9]. The standard technology for monitoring blood glucose concentration is based on blood collection, which a drop of blood is invasively taken by pricking a finger [10, 11]. The collected blood is drawn on a test strip containing glucose oxidase or glucose dehydrogenase to check the glucose concentration [12, 13]. Because blood glucose diagnosis requires repetitive pricking of a finger, the finger-pricking test is usually inconvenient and can cause pain and stress for the patient, as well as the risk of a blood-borne infection [14, 15]. As a result, patient compliance with frequent and routine examinations is often low, increasing the risk of complications [16, 17].

Recently, many studies have been conducted on methods for non-invasively measuring blood glucose using body fluids such as sweat, saliva, urine, and tears [18–21]. Measuring glucose levels in sweat, saliva, or urine is not always accurate and has the potential for toxicity as well as interference from other substances [22–24]. In contrast, tear fluid has been identified as a less interfering non-invasive source for monitoring

glucose levels in diabetes patients [25]. Compared to conventional finger-pricking tests, monitoring tear glucose levels provides a less invasive and continuous monitoring option [26, 27]. To this end, various measurement methods using electric sensors or optical arrangements have been proposed and investigated [27–34]. While continuous monitoring of tear fluids using electronic glucose sensors is a prevalent method, it's noteworthy that some sensors utilized in various devices have faced challenges related to biocompatibility, thereby limiting their in vivo applications, even though there are instances such as contact lens [35, 36], where biocompatible electronic glucose sensors have been effectively developed and utilized. Continuous monitoring of tear fluids using electronic glucose sensors is a popular method, but the sensors used in these devices are generally not biocompatible, limiting their in vivo applications. Additionally, electronic drift in sensor response must be frequently calibrated with fresh blood samples [37]. Electronic glucose systems can also be bulky and complex, and may require excessive electrical components, indicating the need for improvement in device structure and measurement techniques [38].

Optical detection techniques such as surface plasmon resonance (SPR) and fluorescence resonance energy transfer (FRET) have been widely studied for measuring tear glucose concentration [39]. These techniques rely on color changes based on optical indicators that respond to the activation of fluorescently labeled enzymes by

glucose. However, this approach may not be suitable for monitoring tear glucose levels due to several limitations. First of all, an additional high-power light source is required to consistently measure the tear glucose concentration in contact lenses, which may cause pain and discomfort to patients due to eye irritation [26, 40–43]. Additionally, the measurement accuracy and clinical practicality of these techniques can easily be hampered by their high sensitivity to motion, the requirement for a lengthy calibration process, and the short lifetime of fluorophores due to degradation. These limitations lead to inefficiency and lack of suitability of optical techniques for monitoring tear glucose levels, despite their potential *in vivo* and *in situ* benefits.

In this study, we developed a clinically feasible sucking disk-type (SD) strip biosensor containing a sensing paper coated with cerium oxide nanoparticles (CNPs) and glucose oxidase (GOx). This SD strip biosensor can contact the inferior palpebral conjunctiva (IPC) to collect tears without causing eye irritation, facilitating a brief-use, disposable format that enables individuals to perform self-monitoring of glucose levels with ease. The SD strip biosensor produces a distinctive color change within a glucose concentration range of 0~2.5 mM, which encompasses tear glucose levels [44], this SD strip biosensor provides immediate, discernible feedback without necessitating any high-power light sources or complex electrical components. Furthermore, with optimized imaging systems and processing algorithms, we ensure maximal measurement accuracy, reaffirming its applicability and reliability for self-diagnosis. In particular, experimental validation performed using this SD strip biosensor system with tear samples from diabetes-inducing rabbits *in vivo*, and the demonstrated correlation between blood and tear glucose levels, underscore its clinical feasibility and potential as a user-friendly, disposable diagnostic tool.

## Materials and methods

### Materials

Whatman filter paper, cerium (III) nitrate hexahydrate ((Ce(NO<sub>3</sub>)<sub>3</sub>·6H<sub>2</sub>O), sodium hydroxide (NaOH), amino-propyltriethoxysilane (APTS), glucose oxidase, D-(+)-glucose, fluorescein sodium, and phosphate-buffered saline (PBS) were purchased from Sigma Aldrich (St. Louis, MO, USA). All solutions were prepared with ultrapure distilled, deionized water. Materials for 3D printing (VisiJet M3 Crystal) were purchased from 3D Systems (Rock Hill, SC, USA). A glucometer was purchased from Roche Diagnostics (Mannheim, Germany). Ketamine and xylazine were purchased from Yuhan (Seoul, Korea) and Bayer (Leverkusen, Germany), respectively.

### Preparation of the CNPs/APTS/GOx-treated sensing paper

In brief, 1.736 g Ce(NO<sub>3</sub>)<sub>3</sub> was added to 128 mL of NaOH solution (0.4 g NaOH dissolved in 128 mL of distilled water), and the solution was stirred for 48 h. The white precipitate formed after stirring was washed several times with distilled water and collected. The filter paper was shaken in a colloidal CNP solution at several concentrations (0.5, 1, 3, 5, and 10%) for 10 min to ensure that CNP was sufficiently adsorbed. The CNPs-adsorbed filter paper was dried in a 60 °C oven for 1 h. The adsorbed CNPs were stabilized through silicone coating. APTS forms a covalent bond with the hydroxyl group on the filter paper and CNP surface and is coated with silicone. The paper was shaken in a 5% APTS ethanol solution for 10 min and dried in a 60 °C oven for an additional 10 min [45]. Finally, GOx was applied at 11.43 U/cm<sup>2</sup> and dried at room temperature to obtain the CNPs/APTS/GOx-treated sensing paper.

### Fabrication of sucking disk-type (SD) strip biosensor

The SD strip biosensor was designed to contain the sensing paper, onto which tear fluid can be collected and delivered. Thus, the SD strip biosensor was composed of three distinct parts connected in series: tip, channel, and reaction chamber. The tip was rounded with a 3-mm diameter, and an opening was made to form the channel (W×H×L: 2 mm×0.5 mm×0.3 mm) for tear infiltration. At the end of the channel, the reaction chamber (W×H×L: 1 mm×0.5 mm×0.5 mm) was shaped to just fit the sensing paper. A schematic image of a strip-type sensor was drawn with Solidworks (Dassault Systèmes SOLIDWORKS Corp., Waltham, MA, USA). We fabricated the SD strip biosensor with a 3D printer (Projet 3500 HD MAX, 3D Systems, Rock Hill, SC, USA) using VisiJet M3 Crystal (3D Systems, Rock Hill, SC, USA), which is a certified material with known biocompatibility (United State Pharmacopeia Class VI). The illumination model was constructed with an LED spotlight and diffused optics from Edmund Optics. The optical system was constructed with a Sony IMX-128-(L)-AQP CMOS Sensor (Sony Corp., Tokyo, Japan) and objective lens (Edmund Optics, Blackwood, NJ, USA). We removed the shadow and background noise using the algorithm and obtained a color value independent of illuminance through normalization.

### Characterization of the sensing paper

The surface of the sensing paper was characterized using a scanning electron microscope (SEM) (NOVA NANO SEM). X-ray photoelectron spectroscopy (XPS) was used to assess the surface atomic composition of the sensing paper. In addition, energy dispersive spectroscopy (EDS)

mapping was used to confirm the distribution of each element on the sensing paper. In particular, it was analyzed through ICP-MS (NexION 350D) to confirm whether CNPs were present at similar levels in each sensing paper. The sensing paper was prepared in a circular shape with a diameter of 6 mm, and after hydrofluoric acid pretreatment, sampling was performed with the same weight and then analyzed. As a control, filter paper was also produced in a circular shape with a diameter of 6 mm and then analyzed. To confirm that GOx was stably attached to the surface of the sensing paper through an immunofluorescence assay, GOx was determined to be evenly distributed through visualization with MATLAB (Mathworks Inc., Natick, MA, USA). To detect glucose in tears using the sensing paper, different glucose concentrations (0, 0.5, 1, and 2.5 mM) were used to confirm the actuation. A 10  $\mu$ L sample of glucose solution was dropped onto a circular sensing paper with a diameter of 6-mm.

#### **In vitro evaluation of the SD strip biosensor**

To test the sensing paper's reliability to be loaded into the SD strip biosensor, we compared normalized  $b$  values before and after loading. The sensing paper was cut into 1 mm  $\times$  0.5 mm strips, attached to a petri dish, and treated with 0.5  $\mu$ L of glucose solutions with concentrations (0~1.2 mM). On the other hand, the 0.5 mm<sup>2</sup> piece of the sensing paper was loaded in the reaction chamber of the SD strip biosensor, and 0.5  $\mu$ L of glucose at concentrations over the same range (0~1.2 mM) was injected into the channel. After the sensing paper reacted with the glucose solutions for less than 15 min, the yellow color density changed. Then, we acquired the image of the sensing paper with an optical vision system, and the color values of these images were obtained with image processing algorithms.

#### **In vivo evaluation of SD strip biosensor**

Male New Zealand white rabbits (3.0~3.5 kg body weight) were used in this study to evaluate the correlation between tears and blood glucose levels. The experimental protocol was approved by the Institutional Animal Care and Use Committee (IACUC No. 15-0285-C1A0) at the Biomedical Research Institute of Seoul National University Hospital. To induce diabetic condition in rabbits, we intentionally elevated blood glucose levels via subcutaneous injection of a cocktail of 15 mg/kg ketamine and 5 mg/kg xylazine, as reported in previous studies [37, 46, 47]. At 40 and 80 min after the first injection, a cocktail of 7.5 mg/kg ketamine and 2.5 mg/kg xylazine was administered as boosters, respectively. We measured the glucose levels both in tears and in blood at 15, 22, 30, 45, 60, and 90 min after the first injection of anesthesia. To measure

tear glucose level, the tip of the SD strip biosensor was contacted to the IPC of a rabbit eye for 20 s to collect the tear, which infiltrated into the reaction chamber of the SD strip biosensor. In an optical system constructed in the same environment as in vitro, the acquired image and algorithms were used to obtain normalized  $b$  values. At the same sampling times, blood was collected from the rabbit ear vein and measured with a commercially-available glucometer (ACCU-CHEK Performa, Roche Diagnostics, Mannheim, Germany). After multiple applications of the SD strip biosensor, we examined any possible tissue damage to the IPC of the rabbit eyes [46, 48]. To this end, a fluorescein solution (0.25% w/v in PBS, 5  $\mu$ L) was administered topically to the rabbit eye. After 5 min, the eye was thoroughly washed with normal saline. We then obtained a fluorescent image of the IPC, using excitation (475 nm) and emission (542 nm) filters (Thorlabs, Newton, NJ, USA).

#### **Optical monitoring system and normalization**

When a glucose solution reacts in the SD strip biosensor, the yellow intensity of the sensing paper changes at a visible wavelength of about 570 nm. For measuring yellow, we used a white LED light source. The disadvantage of non-uniform intensities of the LED light with a Gaussian distribution was overcome using diffused optics. For color detection, the objective lens was used to enlarge the image of the sensing paper in the SD strip biosensor to  $\times 15$  and acquire the image through the integrated digital camera on the microscope. When the images were transferred to a computer, we obtained color values for the sensing paper through the colorimetric analysis algorithm. Because the color values (RGB) include the brightness of the illumination when capturing an image, they vary depending on illumination. Thus, chromaticity values ( $\rho$ ) independent of brightness are obtained with the following normalization formula:

$$\rho(r, g, b) = \frac{R, G, B}{R + G + B}$$

where  $R$ ,  $G$ , and  $B$  represent the intensity of the red, green, and blue color intensity values on the images, respectively.

#### **Statistics**

All data were presented as mean  $\pm$  S.E.M (standard error of the mean). Statistical analysis was evaluated by Student's  $t$ -tests or one-way analysis of variance (ANOVA).  $P$ -value less than 0.05 was considered a statistically significant value. GraphPad Prism (version 8.3.0; GraphPad Software Inc., San Diego, CA, USA) was used for statistical analyses.

## Results

### Design and characterization of CNPs/APTS/GOx-treated sensing paper

As a glucose sensing material, we used cerium oxide nanoparticles (CNPs) to measure tear glucose concentration after loading on a strip-type sensor. CNPs have been widely used in industry and have recently been studied in biotechnology because of their catalytic activity and low toxicity [49]. CNPs have both  $Ce^{3+}$  and  $Ce^{4+}$  on their surface, and oxygen vacancy because  $Ce^{3+}$  plays an important role in the redox potential of CNPs [50]. When  $Ce^{3+}$  oxidizes to  $Ce^{4+}$ , the colorless CNPs are switched to deep yellow-colored CNPs according to various concentrations of  $H_2O_2$  and glucose (Fig. 1 and Fig. S1). This feature provides colorimetric information that can be obtained easily and relatively cheaply through conventional optical measurements [51, 52]. As a result, CNPs have been studied as a sensing material [53, 54]. We characterized the CNPs with high-resolution transmission electron

microscopy (HR-TEM) images, suggesting that the synthesized CNPs (6 nm in diameter) had a unique lattice structure on their surface (Fig. S2). The surface of CNPs-treated sensing paper was visualized by using scanning electron microscopy (SEM) (Fig. 1b and Fig. S3).

To characterize the sensing paper, we analyzed the respective elemental composition and chemical state of the paper surface by using X-ray photoelectron spectroscopy (XPS) and energy dispersive spectroscopy (EDS) mapping (Fig. 2). We performed EDS mapping of the CNPs and 3-aminopropyltriethoxysilane (APTS)-treated filter paper (Figs. S4–S6). Because the filter paper was made of cellulose fiber, the O1s and C1s peaks appeared in the XPS spectrum (Fig. 2a-I, II, b and Fig. S7). After treatment of CNP solution (3% w/v), the Ce3d peak appeared in XPS spectra (Fig. 2a-IV, c and Fig. S8). We treated APTS to stabilize the CNPs adsorbed on the filter paper. APTS reacts with the hydroxyl groups present on the surfaces of the filter paper and CNP to form

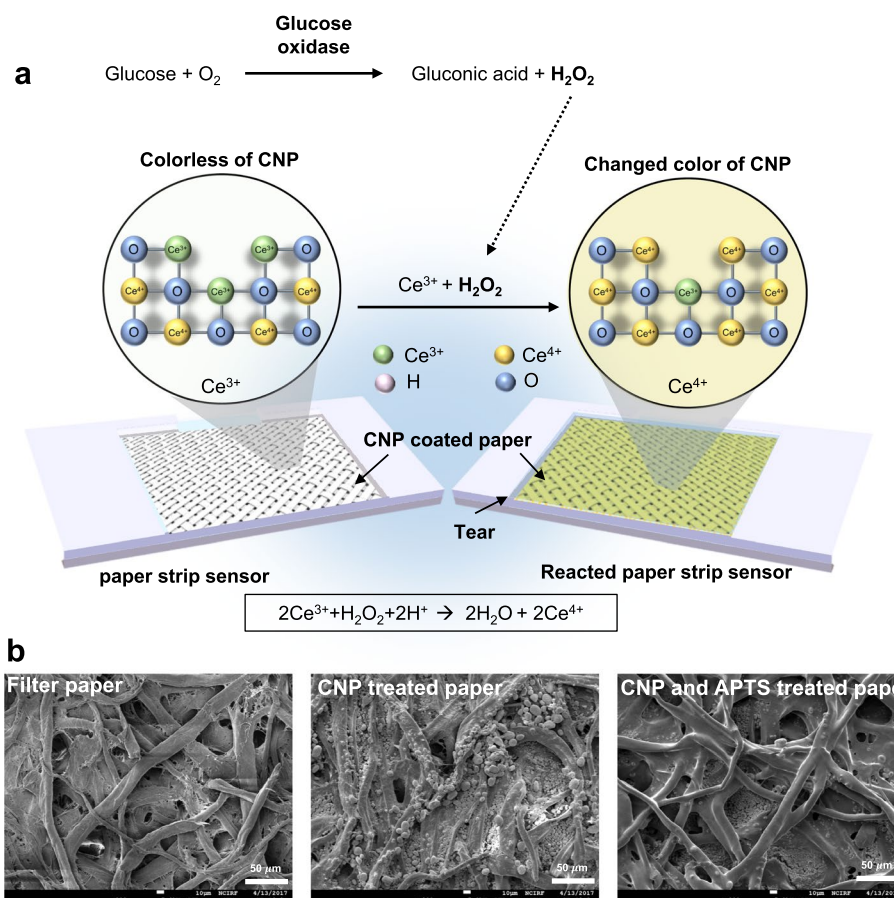


**Fig. 1** Schematic illustration of the sensor paper treated with cerium oxide nanoparticle (CNP), 3-aminopropyltriethoxysilane (APTS), and glucose oxidase (GOx). **a** Reaction scheme of the immobilized CNP, GOx, and glucose on the sensing paper. The sensing paper color is changed in response to tear glucose concentration from colorless  $Ce^{3+}$  (before reaction) to yellow  $Ce^{4+}$  (after reaction) due to the oxidation of cerium ions. **b** Captured scanning electron microscopy (SEM) images of filter paper, filter paper treated with CNPs, and filter paper treated with CNPs/APTS

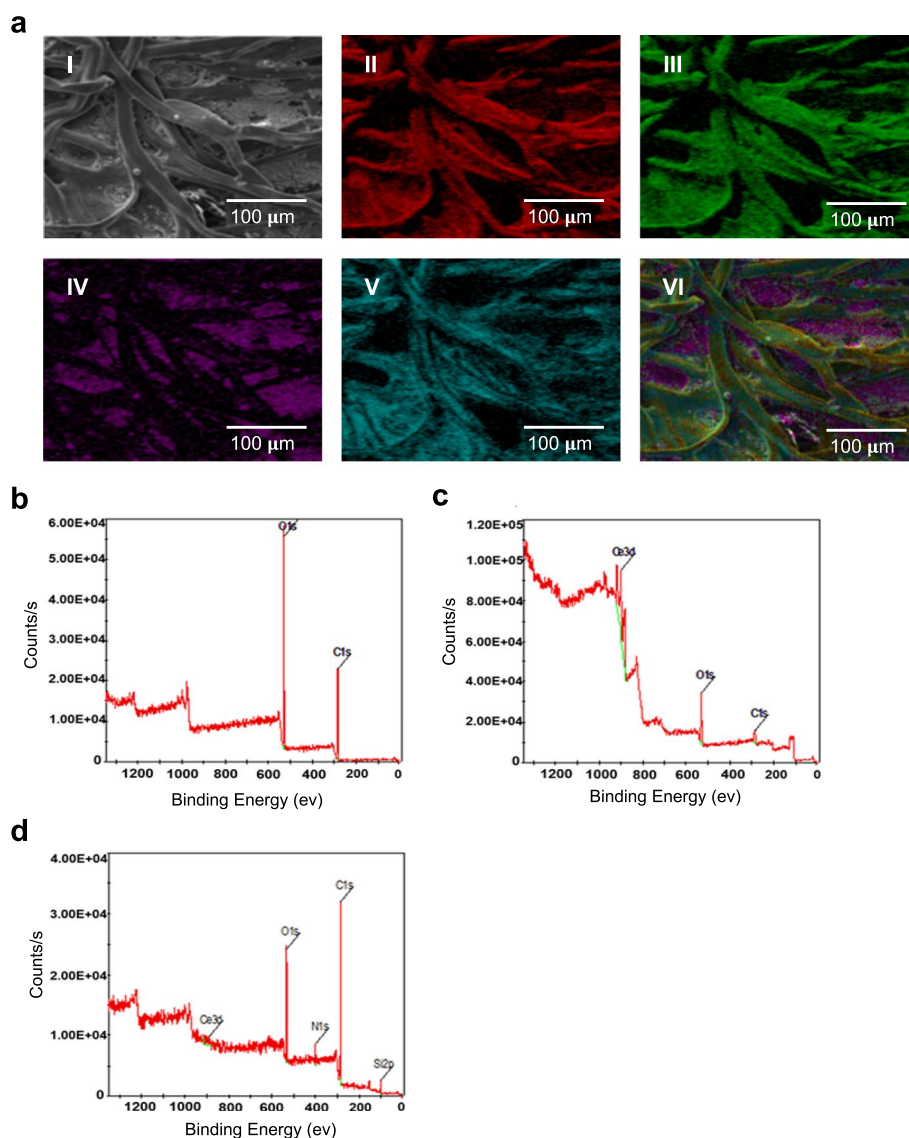


**Fig. 2** X-ray photoelectron spectroscopy (XPS) characterization and energy dispersive spectroscopy (EDS) mapping with scanning electron microscopy (SEM) of sensing paper treated with CNP and APTS. **a**-I SEM images of CNP- and APTS-treated filter paper. **a**-II – **a**-VI exhibit the element mapping of carbon (red, II), oxygen (green, III), cerium (purple, IV), and silicon (cyan, V), in that order. **a**-VII Merged EDS maps of CNP- and APTS-treated filter paper. **b** XPS spectra of filter paper made of cellulose fiber. **c** XPS spectra of CNP-treated filter paper. The spectra represented Ce3d peak, meaning CNP. **d** XPS spectra of CNP and APTS-treated filter paper. The spectra represented Si2p peak, meaning APTS

a covalent bond. After further treatment of APTS, new peaks corresponding to N1s and Si2p appeared (Fig. 2a-V, d and Fig. S9). These XPS and EDS mappings indicate that CNPs and APTS were broadly coated on the whole surface area of the sensing paper. Additionally, to determine whether there was a change in the color reaction of CNPs covalently bonded with APTS, the color development reaction was checked before and after APTS treatment. As a result, there was no significant change in the color reaction before and after APTS treatment (Figure S10). After the treatment of CNPs/APTS on the surface

of the sensing paper, the glucose oxidase (GOx) enzyme was finally treated onto the CNP/APTS-treated sensing paper without any chemical cross-linking. Immunofluorescence assay was used to demonstrate the stable immobilization of GOx on the CNP/APTS-treated sensing paper (Fig. 3a). To quantitatively analyze GOx treatment on the sensing paper, we developed image processing algorithms to extract the regions of interest (ROI) within the image (Fig. S11). The quantified uniformity, illustrated by a standard deviation of  $90.5 \pm 0.03\%$  for CNPs/APTS-treated paper and  $99.2 \pm 0.99\%$  for CNPs/APTS/

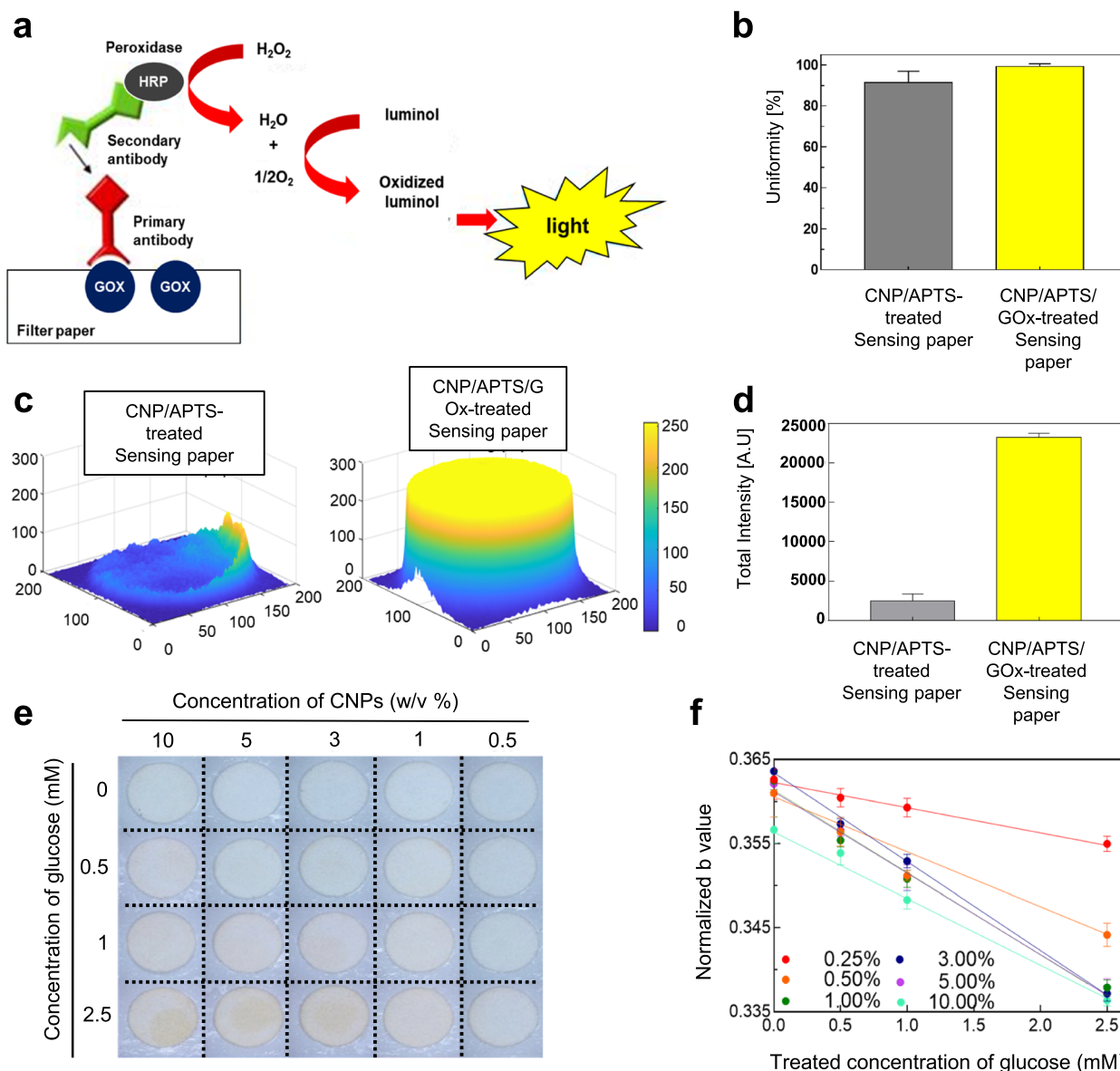


**Fig. 3** Characterization of the CNPs/APTS/GOx-treated sensing paper. **a** Schematic diagram of an immunofluorescence assay to check the uniform distribution of GOx on the sensing paper. The primary antibody of GOx and secondary antibody were reacted with the sensing paper. **b** Calculated uniformity to verify the uniform distribution of GOx. **c** The MATLAB 3D image to plot the uniformity of CNPs/APTS-treated paper and CNPs/APTS/GOx-treated sensing paper. **d** The total intensity to confirm the uniform distribution of CNPs/APTS-treated paper and CNPs/APTS/GOx-treated sensing paper. **e** Optimization of the concentration of CNPs (0.5, 1, 3, 5, and 10 w/v%) at different glucose concentrations (0, 0.5, 1, and 2.5 mM) for optimal sensitivity of glucose. **f** Linear regression curves of normalized b value from (e) result. Data were presented as the mean  $\pm$  standard deviation ( $n=5$ )

GOx-treated sensing paper in Fig. 3b, underscores the high uniformity and replicability in our fabrication process, demonstrating the reliable distribution of CNPs and GOx throughout the sensing paper. In addition, the 10-fold higher fluorescence signal with  $23,322 \pm 400.3$  A.U was equally detected on the whole area of CNPs/APTS/GOx-treated sensing paper than CNP/APTS treated sensing paper with  $2,512.8 \pm 712.8$  A.U (Fig. 3c

and d), suggesting that a higher density of GOx enzyme was consistently and evenly coated on the entire area of CNPs/APTS-treated sensing paper. The uniform distribution of GOx on the sensing paper played an important role in the accurate and reliable detection of the target molecule in the sample, thus ensuring the reproducibility of the sensing performance. Next, we optimized the concentration and volume of CNPs to maximize the

sensitivity of various concentrations of glucose on the sensing paper. The color change was not significant at low CNP concentrations (0.5% w/v), whereas the base color of the paper was too yellow to detect a change in color at high CNP concentrations (10% w/v) (Fig. 3e and g). ICP-MS analysis was performed to quantify the CNPs present in the sensing paper. The sensing paper was sampled with the same weight (15 g) after hydrofluoric acid pretreatment, and the amount of CNPs present in it was measured. As a result, the average and standard deviation of the amount of CNP present in the sample were measured to be 6453.7 ppb and 416.2 ppb, respectively (Table S1). Based on this result, the uniformity is 92.4%, which means that the CNPs present in the sensing paper are evenly distributed. Additionally, our study highlighted the importance of macro-scale uniformity in CNP distribution. We utilized an RGB camera to capture the entire sensor area, effectively balancing practical application with in-depth analysis. Despite possible height variations due to the fibrous nature of the filter paper, our sensor was designed to reliably detect uniform signals across the entire area at a macro-scale level in Fig. 3c. To quantitatively analyze the color change, we optimized the image processing algorithm (Fig. S12a). This algorithm could automatically calculate the degree of color change, which is proportional to the concentration of glucose present in the sample. Because the complementary color (blue) of the reflected color (yellow) is more sensitive than other reflected green and red colors, the glucose concentration was analyzed as blue color with the normalization formula (Fig. S12b). By using this image processing algorithm, the optimal concentration of CNP was 3% (w/v) to detect glucose concentration on the CNPs/APTS/GOx-treated sensing paper, showing the largest and most significant slope in the linear regression graph ( $R^2=0.998$ ) (Fig. 3f and h).

#### **Fabrication of sucking disk-type (SD) strip biosensor with the CNPs/APTS/GOx-treated sensing paper**

The design of the strip-type biosensor needs to be well-suited for collecting and delivering tear fluid to the sensing paper. To properly collect and deliver tear fluid to the sensing paper, we designed the sucking disk-type (SD) strip biosensor consisting of a tip, channel, and reaction chamber connected in series, which could easily be manufactured by using a 3-dimensional printer device (Fig. 4a). This is important because any damage to the eye surface can cause discomfort and may lead to complications such as infection or inflammation [43, 55, 56]. The rounded sucking disk tip can help to distribute the pressure evenly during the collection of tears at the inferior palpebral conjunctiva (IPC) without any eye irritation. In addition, the rectangular-shaped channel is adopted

to effectively suck tears by increasing capillary pressure [57]. Next, the prepared sensing paper was cut to insert into the reaction chamber of the SD strip biosensor. After that, we tested the color changes in the reaction chamber of the SD strip biosensor before and after the treatment of glucose (1.2 mM, 0.5  $\mu$ L) (Fig. 4c). In this process, we newly manufactured the tailored optical system to exactly analyze the color change of CNPs/APTS/GOx-treated sensing paper in the reaction chamber with a tiny window (1 mm  $\times$  0.5 mm) (Fig. 4b). Also, we optimized the normalized image process to quantitatively analyze the color change in the reaction chamber with a tiny window (Fig. S12a, Fig. 4c, and Fig. S13). The original and normalized image could reflect the different glucose concentrations. Finally, we compared the color variation of the sensing paper before and after being loaded into the SD strip biosensor at various concentrations of glucose (0.5  $\mu$ L) (Fig. 4d). In both groups, they were not significantly different, both showing that the normalized b values proportionally decreased as glucose concentration proportionally increased ( $R^2=0.9716$ ). This correlation test showed that the sensing papers had an almost consistent profile, suggesting that the function was unchanged after the sensing paper was loaded into the SD strip biosensor. In addition, we have confirmed the color variation of SD strip biosensor at low glucose concentrations (0.001, 0.005, 0.01, and 0.1 mM). Notably, a significant colorimetric change was observed at 0.1 mM, as confirmed by our optical monitoring system ( $p < 0.05$  mM), as depicted in Supporting Information Fig. S14.

#### **In vivo evaluation of the SD strip biosensor in a diabetic rabbit model**

The actuation of the SD strip biosensor was evaluated in the inferior palpebral conjunctiva (IPC) of a diabetic rabbit model (Fig. 5a, arrow). When the SD strip biosensor was in contact with the IPC, the tear was successfully absorbed through the channel and diffused into the reaction chamber with the CNPs/APTS/GOx-treated sensing paper. The entire working process of the SD strip biosensor shown in Movie S1. To evaluate the damage to the eye surface after the in vivo experiments, the IPC of the eye of the rabbit was stained with fluorescein (Fig. 5b). The experiment revealed no staining of tissue, indicating no IPC damage even after multiple contacts with the SD strip biosensor (Fig. S15a). In contrast, when the IPC was contacted one time with a glass capillary tube that is conventionally used for tear collection, a fluorescence-stained region was clearly observed due to tissue damage [46, 56]. Quantitative measurements of the damaged area with the developed image processing algorithm showed a significant difference between the glass capillary tube and the SD strip biosensor (Fig. S1b). In addition, this SD



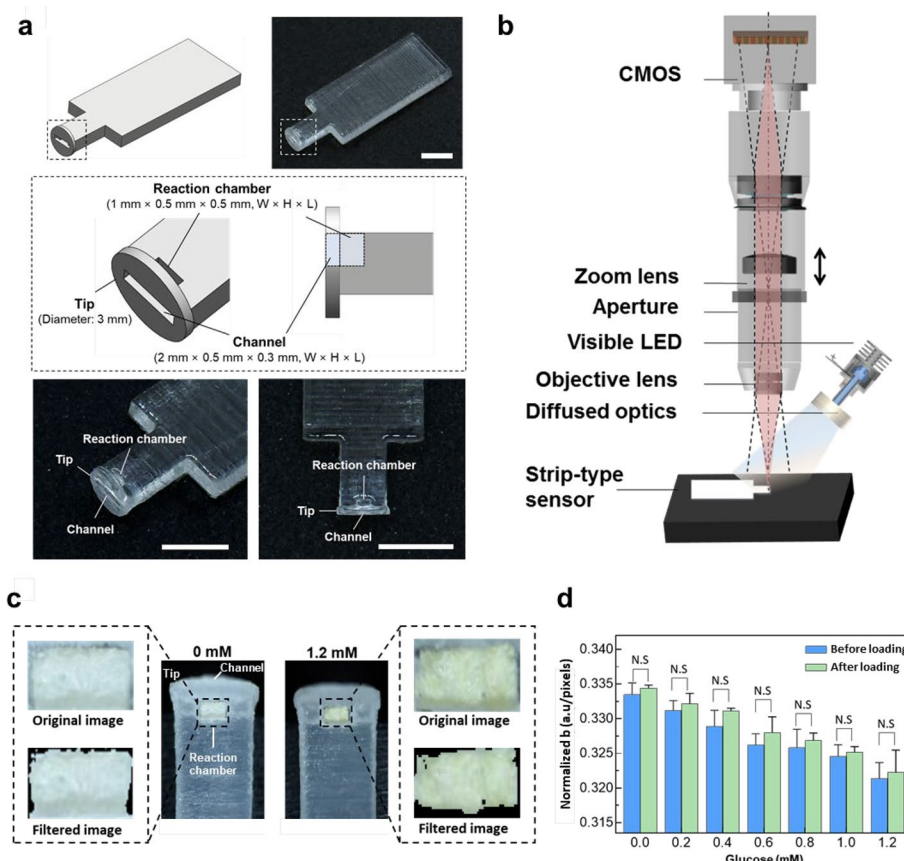


**Fig. 4** Actuation of sucking disk-type (SD) strip biosensor embedded with CNPs/APTS/GOx-treated sensing paper. **a** Schematic and optical images of the sucking disk-type (SD) strip sensor. The CNPs/APTS/GOx-treated sensing paper was inserted in the reaction chamber. Scale bar = 5 mm. **b** Schematic image of the optical system to capture the colorimetric images of the CNPs/APTS/GOx-treated sensing paper in the reaction chamber with a tiny window to the SD strip biosensor. **c** Real image (original) and normalized image (filtered) of the sensing paper in the reaction chamber of SD strip biosensor before and after treatment of glucose solution (1.2 mM). The normalized image was obtained with an image processing algorithm. **d** Correction test for comparison of sensing paper performance. We monitored color variation by calculating the normalized blue (normalized b) value between sensing paper before and after being loaded into the SD strip biosensor. Data were presented as the mean ± standard deviation (n = 5). NS: No significant difference

strip biosensor does not require a huge volume of tears because the channel of the SD strip biosensor is designed to possess a high capillary pressure with minimal dead volume (Fig. 4a). The channel of the SD strip biosensor had a rectangular cross-section and was 0.5 mm in height, 2 mm in width, and 0.3 mm in length. The reaction chamber was shaped to just fit the sensing paper at 0.5 mm<sup>2</sup>. In this way, a fixed volume (0.5 μL) of tear fluid could be collected to react with the sensing paper, which is smaller than the total volume of basal tear fluid available in the preocular space [58].

In the diabetes-inducing rabbit animal model, tear fluid was collected within a few seconds and measured at scheduled times using the SD strip biosensor while the blood glucose level was also measured concurrently (Fig. 5c). The normalized b values obtained from each sampled measurement decreased as the blood glucose

level increased. When the normalized b value was converted to the tear glucose level through the measurement index described above, there was a strong correlation between tear and blood glucose levels during the diabetes-inducing procedure in rabbits (Fig. 5d) [26, 59]. The glucose elevation profiles of the rabbits in a fasting state were almost consistent for all individuals, with each rabbit reaching glucose levels within a diabetic range [10, 27]. Throughout this range, the SD strip biosensor successfully estimated glucose levels in tears of the diabetic rabbits. As the sensor herein is designated for sampled measurements, the reproducibility of the sensor performance is expected to be maintained within the tested range of blood glucose level. Figure 5e shows the linear relationship between glucose levels in tears and in blood ( $R^2=0.95$ ). Again, a strong correlation was observed between the normalized b value and blood glucose level

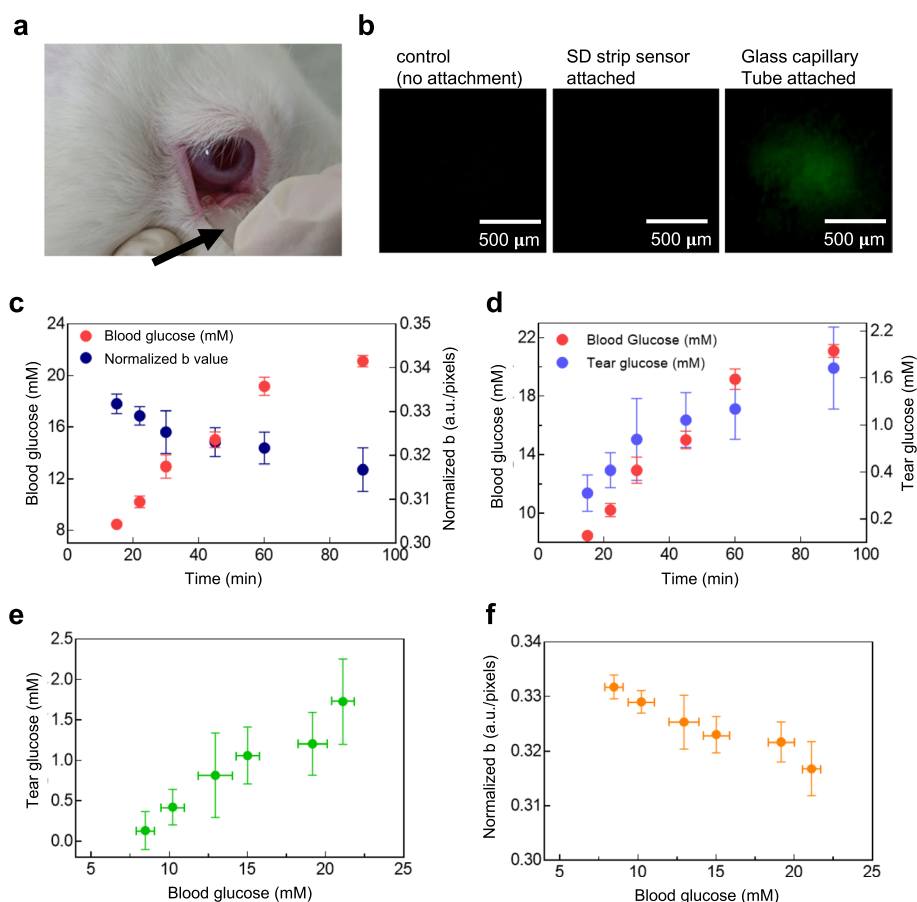


**Fig. 5** Blood glucose prediction by using measurement of tear glucose levels with the SD strip biosensor. **a** Touch of SD strip biosensor in the inferior palpebral conjunctiva (IPC) of a diabetic rabbit model. Arrow: SD strip biosensor. **b** Monitoring surface damage to the eye during tear collection with a glass capillary tube or SD strip biosensor. Eye damage was visualized after instillation into the rabbit IPC with 5  $\mu\text{L}$  of 0.25% w/v fluorescein sodium solution. Fluorescein image: eye damage. Fluorescent region indicates eye tissue damage. **c** The comparison between the normalized b values and blood glucose concentration at each time point. At each sampling time, five rabbits were tested and a single measurement was performed for each animal. Data were presented as the mean  $\pm$  standard deviation ( $n=5$ ). **d** The comparison between the tear glucose and blood glucose concentration at each time point. Data were presented as the mean  $\pm$  standard deviation ( $n=5$ ). **e** A linear correlation between blood and tear glucose levels. Data were presented as the mean  $\pm$  standard deviation ( $n=5$ ). **f** A linear correlation between blood glucose levels and normalized b values. Data were presented as the mean  $\pm$  standard deviation ( $n=5$ )

(Fig. 5f). The observation shows the applicability of the current technique for the management of diabetes and indicates a correlation between tear glucose and blood glucose level as shown in previous studies [26, 59]. While further in vivo validation is needed to improve clinical use, our study demonstrates the potential for safely and accurately measuring a wide range of glucose concentrations in tears by using SD strip biosensor.

**Discussion**

This study presents a comprehensive approach to tear glucose monitoring by combining the advantageous properties of cerium oxide nanoparticles, precise immobilization of glucose oxidase, advanced image processing

algorithms, and a user-friendly biosensor design. The results underscore the potential for a fully automated and safe tear glucose monitoring system that could significantly contribute to diabetes management in the clinical setting.

The CNPs-based sensing paper developed in this study offers several advantages for glucose sensing applications. The colorimetric response of CNPs to glucose concentration changes provides a simple and visual method for detecting glucose levels. Characterization of the CNPs-treated sensing paper was carried out through a combination of high-resolution transmission electron microscopy (HR-TEM) and scanning electron microscopy (SEM). These techniques provided insight into the

unique lattice structure of the synthesized CNPs and visualized the surface of the sensing paper. This characterization not only confirmed the successful synthesis of the CNPs but also validated their uniform distribution on the sensing paper, a pivotal factor for achieving consistent and reliable sensing performance. The functionalization of the sensing paper involved a sequential treatment of CNPs and 3-aminopropyltriethoxysilane (APTS), followed by the immobilization of glucose oxidase (GOx) without the need for chemical cross-linking. The use of immunofluorescence assay provided robust evidence of the stable and uniform immobilization of GOx on the CNP/APTS-treated sensing paper. To quantitatively analyze the GOx distribution, sophisticated image processing algorithms were developed to accurately extract regions of interest (ROIs). The even distribution of GOx across the entire surface of the CNP/APTS-treated sensing paper is a key factor in achieving consistent and reproducible sensing outcomes. The optimization of CNP concentration, determined to be 3% (w/v), exemplifies the intricate balance between color change intensity and sensitivity. The developed image processing algorithm, based on the complementary color (blue) of the reflected color (yellow), provides a robust approach for quantitatively assessing glucose concentrations on the CNPs/APTS/GOx-treated sensing paper. The high linearity achieved ( $R^2=0.998$ ) in the glucose concentration detection range underscores the reliability and accuracy of the developed biosensor. From a clinical perspective, the detection of hypoglycemia holds paramount importance for patients with diabetes mellitus, given the potential for serious complications that often necessitate emergency medical attention. Our benchtop study has demonstrated the technical feasibility of quantifying tear glucose levels below 0.2 mM, with the lowest detection limit being 0.1 mM (Refer to Supporting Information Fig. S14). This observation suggests the potential applicability of our current technique in detecting hypoglycemia.

The sucking disk-type (SD) strip biosensor fabrication, specifically designed to collect and deliver tear fluid to the sensing paper, marks a significant advancement in tear glucose monitoring. The ease of manufacturing this biosensor, using a 3-dimensional printer, provides economic advantages compared to conventional tear glucose biosensors. Importantly, the SD strip biosensor's design considers the well-being of the eye surface, minimizing potential damage and discomfort during tear collection. The successful evaluation of the SD strip biosensor in a diabetic rabbit model further substantiates its potential for practical application. The absence of tissue damage, even after multiple contacts with the biosensor, highlights its safety. The strong correlation observed between tear glucose and blood glucose levels in the rabbit model

emphasizes the biosensor's reliability and potential clinical utility.

## Conclusions

In conclusion, we processed the CNPs/APTS/GOx-treated sensing paper. Then the sensing paper was easily mounted in the reaction chamber of the SD strip biosensor manufactured with a 3-dimensional printer. Because the sensing paper and the SD strip biosensor can be manufactured with facile processes, this SD strip biosensor system is economically advantageous compared with other tear glucose biosensors. In addition, this SD strip biosensor system was successfully evaluated with the optimized image algorithm in the diabetes-inducing rabbit model. Collectively, this SD strip biosensor system can be in a significant step toward developing a fully automated instrument for tear glucose monitoring in diabetes patients.

## Abbreviations

SD	Sucking disk-type
CNP	Cerium Oxide Nanoparticle
GOx	Glucose Oxidase
BGST	Blood glucose self-testing
SPR	Surface Plasmon Resonance
FRET	Fluorescence Resonance Energy Transfer
IPC	Inferior Palpebral Conjunctiva
APTS	Aminopropyltriethoxysilane
PBS	Phosphate-Buffered Saline
NaOH	Sodium hydroxide
SEM	Scanning Electron Microscope
HR-TEM	High-resolution transmission electron microscopy
XPS	X-ray Photoelectron Spectroscopy
EDS	Energy Dispersive Spectroscopy
ROI	Regions of Interest

## Supplementary Information

The online version contains supplementary material available at <https://doi.org/10.1186/s40824-023-00469-5>.

**Additional file 1: Movie S1.** The Entire working process of SD strip biosensor. **Table S1.** The concentration of cerium in samples. **Fig. S1.** Color change showing that CNPs reacted with  $H_2O_2$  or glucose solution. **Fig. S2.** HR-TEM image with a magnification of  $\times 200,000$  of CNPs, showing the distinct structure of the nanoparticles. **Fig. S3.** SEM image of CNPs-treated sensing paper (a) and CNPs/APTS-treated sensing paper. **Fig. S4.** EDS mapping of bare sensing paper. **Fig. S5.** EDS mapping of CNP-treated sensing paper. **Fig. S6.** EDS mapping of CNPs/APTS-treated sensing paper. **Fig. S7.** XPS survey spectra of bare sensing paper. **Fig. S8.** XPS survey spectra of CNPs-treated sensing paper. **Fig. S9.** XPS survey spectra of CNPs/APTS-treated sensing paper. **Fig. S10.** Comparison of normalized b values before and after APTS treatment in CNPs conjugation at the different concentration of  $H_2O_2$ . N.S indicates no significant difference. **Fig. S11.** The overall process for calculating total intensity and uniformity with an immunofluorescence image (inverted image) of CNPs/APTS-treated and CNPs/APTS/GOx-treated sensing paper. (a) Image processing algorithm to evaluate the CNPs/APTS-treated sensing paper and CNPs/APTS/GOx-treated sensing paper. (b) The overall image process for calculating the effect of GOx treatment on the CNPs/APTS-treated sensing paper. **Fig. S12.** The comparison and image processing between original RGB and normalized rgb image. **Fig. S13.** The overall process to estimate the color

change of the sensing paper in the action chamber of SD strip biosensor in response to tear glucose concentration. **Fig. S14.** Assessment of the Limit of Detection (LOD) for Low Glucose Concentrations. **Fig. S15.** Image analysis of eye damage using fluorescent dye after touching the SD strip biosensor to the IPC of the rabbit eye.

#### Acknowledgements

Not applicable.

#### Authors' contributions

SP and DYN performed the Conceptualization, Methodology, Validation, Formal analysis, Investigation, Writing – original draft. HJJ and JHH performed Methodology, Validation, Formal analysis, Data curation, Visualization, Writing – original draft, Writing – review & editing. DJ, JH, YSP, and YGH performed Methodology, Investigation. YBC performed Conceptualization, Supervision, Writing – review & editing, Project administration, Funding acquisition. DYL performed Conceptualization, Supervision, Writing – review & editing, Project administration, Funding acquisition. All authors read and approved the final manuscript.

#### Funding

This research was supported by the National Research Foundation of Korea (NRF) grant funded by the Korean government (MSIT) (NRF-2015M3A9E2030125, NRF-2020R1A2C3005834, NRF-2022R1A4A1030421, and RS-2023-00213379). This research was also financially supported by the Ministry of Trade, Industry and Energy (MOTIE) and Korea Institute for Advancement of Technology (KIAT) through the International Cooperative R&D program (Project No. P0017190).

#### Availability of data and materials

The datasets used and/or analyzed during the current study are available from the corresponding author on reasonable request.

#### Declarations

##### Ethics approval and consent to participate

Hospital This study does not involve human participants, human data, or human tissue. This study involved experimental animals. The experimental protocol was approved by the Institutional Animal Care and Use Committee (IACUC No. 15-0285-C1A0) at the Biomedical Research Institute of Seoul National University Hospital.

##### Consent for publication

Not applicable.

##### Competing interests

The authors declare no conflict of interest.

##### Author details

<sup>1</sup>Department of Bioengineering, College of Engineering, and BK FOUR Biopharmaceutical Innovation Leader for Education and Research Group, Hanyang University, 222 Wangsimni-Ro Seongdong-Gu, Seoul 04763, Republic of Korea.

<sup>2</sup>College of Engineering, Interdisciplinary Program in Bioengineering, Seoul National University, 1 Gwanak-Ro Gwanak-Gu, Seoul 08826, Republic of Korea.

<sup>3</sup>Department of Mechanical and Biomedical Engineering, Kangwon National University, 1 Gangwondaehak-Gil, Chuncheon 24341, Republic of Korea.

<sup>4</sup>Department of Physics, College of Natural Sciences, Hanyang University, 222 Wangsimni-Ro Seongdong-Gu, Seoul 04763, Republic of Korea. <sup>5</sup>Department of Biomedical Engineering, Seoul National University College of Medicine, 101 Daehak-Ro Jongno-Gu, Seoul 03080, Republic of Korea. <sup>6</sup>Institute of Medical & Biological Engineering, Medical Research Center, Seoul National University, 101 Daehak-Ro Jongno-Gu, Seoul 03080, Republic of Korea. <sup>7</sup>Institute of Nano Science and Technology (INST) and Institute for Bioengineering and Biopharmaceutical Research (IBBR), Hanyang University, 222 Wangsimni-Ro Seongdong-Gu, Seoul 04763, Republic of Korea. <sup>8</sup>Elixir Pharmatech Inc, 222 Wangsimni-Ro Seongdong-Gu, Seoul 04763, Republic of Korea.

Received: 24 August 2023 Accepted: 24 November 2023

Published online: 18 December 2023

#### References

- Cole JB, Florez JC. Genetics of diabetes mellitus and diabetes complications. *Nat Rev Nephrol.* 2020;16(7):377–90.
- Nickerson HD, Dutta S. Diabetic complications: current challenges and opportunities. *J Cardiovasc Transl Res.* 2012;5(4):375–9.
- Clark CM, Fradkin JE, Hiss RG, Lorenz RA, Vinicor F, Warren-Boulton E. Promoting early diagnosis and treatment of type 2 diabetes: the National Diabetes Education Program. *JAMA.* 2000;284(3):363–5.
- Caswell M, Brown D, Frank J, Wallace JF, Pardo S. Accuracy and user performance evaluation of a blood glucose monitoring system which wirelessly transmits results to compatible insulin pumps. *Curr Med Res Opin.* 2020;36(5):757–64.
- Rhew K, Cae YJ, Chang JE. Progress and recent trends in photodynamic therapy with nanoparticles. *J Pharm Investig.* 2022;52(5):587–99.
- Revuri V, Mondal J, Mohapatra A, Rajendrakumar KS, Surwase SS, Park IK, Park J, Lee YK. Catalase-mimicking synthetic nano-enzymes can reduce lipopolysaccharide-induced reactive oxygen generation and promote rapid detection of hydrogen peroxide and L-cysteine. *J Pharm Investig.* 2022;52(6):749–64.
- Jha P, Singh A, Sharma PK, Porwal O, Fuloria NK. Graphene-based nano-material system: a boon in the era of smart nanocarriers. *J Pharm Investig.* 2021;51:245–80.
- Lee JS, Youn YH, Kwon IL, Ko NR. Recent advances in quantum dots for biomedical applications. *J Pharm Investig.* 2018;48:209–14.
- Rebel A, Rice MA, Fahy BG. Accuracy of point-of-care glucose measurements. *J Diabetes Sci Technol.* 2012;6(2):396–411.
- Valeri C, Pozzilli P, Leslie D. Glucose control in diabetes. *Diabetes Metab Res Rev.* 2004;20(Suppl 2):S1–8.
- Meetoo DD, McAllister G, West A. Assessing glycaemic control: self-monitoring of blood glucose. *Br J Nurs.* 2011;20(15):919–20, 922, 924–5.
- Yoo EH, Lee SY. Glucose biosensors: an overview of use in clinical practice. *Sensors (Basel).* 2010;10(5):4558–76.
- Wang J. Glucose biosensors: 40 years of advances and challenges. *Electroanal.* 2001;13(12):983–8.
- Heinemann L. Finger pricking and pain: a never ending story. *J Diabetes Sci Technol.* 2008;2(5):919–21.
- Klonoff DC, Perz JF. Assisted monitoring of blood glucose: special safety needs for a new paradigm in testing glucose. *J Diabetes Sci Technol.* 2010;4(5):1027–31.
- Lane JD, Krumholz DM, Sack RA, Morris C. Tear glucose dynamics in diabetes mellitus. *Curr Eye Res.* 2006;31(11):895–901.
- Kim J, Campbell AS, Wang J. Wearable non-invasive epidermal glucose sensors: A review. *Talanta.* 2018;177:163–70.
- Liu C, Sheng Y, Sun Y, Feng J, Wang S, Zhang J, Xu J, Jiang D. A glucose oxidase-coupled DNAzyme sensor for glucose detection in tears and saliva. *Biosens Bioelectron.* 2015;70:455–61.
- Karpova EV, Shcherbacheva EV, Galushin AA, Vokhmyanina DV, Karyakina EE, Karyakin AA. Noninvasive Diabetes Monitoring through Continuous Analysis of Sweat Using Flow-Through Glucose Biosensor. *Anal Chem.* 2019;91(6):3778–83.
- Lin PH, Sheu SC, Chen CW, Huang SC, Li BR. Wearable hydrogel patch with noninvasive, electrochemical glucose sensor for natural sweat detection. *Talanta.* 2022;241:123187.
- Lee T, Kim I, Cheong DY, Roh S, Jung HG, Lee SW, Kim HS, Yoon DS, Hong Y, Lee G. Selective colorimetric urine glucose detection by paper sensor functionalized with polyaniline nanoparticles and cell membrane. *Anal Chim Acta.* 2021;1158:338387.
- Reddy VS, Agarwal B, Ye Z, Zhang C, Roy K, Chinnappan A, Narayan RJ, Ramakrishna S, Ghosh R. Recent Advancement in biofluid-based glucose sensors using invasive, minimally invasive, and non-invasive technologies: a review. *Nanomaterials (Basel).* 2022;12(7):1082.
- Lee H, Hong YJ, Baik S, Hyeon T, Kim DH. Enzyme-Based Glucose Sensor: From Invasive to Wearable Device. *Adv Healthc Mater.* 2018;7(8):e1701150.
- Shu Y, Su T, Lu Q, Shang Z, Xu Q, Hu X. Highly stretchable wearable electrochemical sensor based on Ni-Co MOF nanosheet-decorated Ag/rGO/PU fiber for continuous sweat glucose detection. *Anal Chem.* 2021;93(48):16222–30.

25. Tang L, Chang SJ, Chen CJ, Liu JT. Non-invasive blood glucose monitoring technology: a review. *Sensors* (Basel). 2020;20(23):6925.
26. Baca JT, Finegold DN, Asher SA. Tear glucose analysis for the non-invasive detection and monitoring of diabetes mellitus. *Ocul Surf*. 2007;5(4):280–93.
27. Keum DH, Kim SK, Koo J, Lee GH, Jeon C, Mok JW, Mun BH, Lee KJ, Kamrani E, Joo CK, Shin S, Sim JY, Myung D, Yun SH, Bao Z, Hahn SK. Wireless smart contact lens for diabetic diagnosis and therapy. *Sci Adv*. 2020;6(17):eaba3252.
28. Yao H, Shum AJ, Cowan M, Lahdesmaki I, Parviz BA. A contact lens with embedded sensor for monitoring tear glucose level. *Biosens Bioelectron*. 2011;26(7):3290–6.
29. Chu MX, Miyajima K, Takahashi D, Arakawa T, Sano K, Sawada S, Kudo H, Iwasaki Y, Akiyoshi K, Mochizuki M, Mitsubayashi K. Soft contact lens biosensor for in situ monitoring of tear glucose as non-invasive blood sugar assessment. *Talanta*. 2011;83(3):960–5.
30. Kim J, Kim M, Lee MS, Kim K, Ji S, Kim YT, Park J, Na K, Bae KH, Kyun Kim H, Bien F, Young Lee C, Park JU. Wearable smart sensor systems integrated on soft contact lenses for wireless ocular diagnostics. *Nat Commun*. 2017;8:14997.
31. Jeon HJ, Kim S, Park S, Jeong IK, Kang J, Kim YR, Lee DY, Chung E. Optical assessment of tear glucose by smart biosensor based on nanoparticle embedded contact lens. *Nano Lett*. 2021;21(20):8933–40.
32. Jeon HJ, Kim HS, Chung E, Lee DY. Nanozyme-based colorimetric biosensor with a systemic quantification algorithm for noninvasive glucose monitoring. *Theranostics*. 2022;12(14):6308–38.
33. Kim S, Jeon HJ, Park S, Lee DY, Chung E. Tear glucose measurement by reflectance spectrum of a nanoparticle embedded contact lens. *Sci Rep*. 2020;10(1):8254.
34. Park S, Hwang J, Jeon HJ, Bae WR, Jeong IK, Kim TG, Kang J, Han YG, Chung E, Lee DY. Cerium oxide nanoparticle-containing colorimetric contact lenses for noninvasively monitoring human tear glucose. *ACS Appl Nano Mater*. 2021;4(5):5198–210.
35. Kim SK, Lee GH, Jeon C, Han HH, Kim SJ, Mok JW, Joo CK, Shin S, Sim JY, Myung D. Bimetallic nanocatalysts immobilized in nanoporous hydrogels for long-term robust continuous glucose monitoring of smart contact lens. *Adv Mater*. 2022;34(18):2110536.
36. Han HH, Kim S-K, Kim S-J, Choi I, Mok JW, Joo C-K, Shin S, Hahn SK. Long-term stable wireless smart contact lens for robust digital diabetes diagnosis. *Biomaterials*. 2023;302:122315.
37. Peng B, Lu J, Balijepalli AS, Major TC, Cohan BE, Meyerhoff ME. Evaluation of enzyme-based tear glucose electrochemical sensors over a wide range of blood glucose concentrations. *Biosens Bioelectron*. 2013;49:204–9.
38. So CF, Choi KS, Wong TK, Chung JW. Recent advances in noninvasive glucose monitoring. *Med Devices* (Auckl). 2012;5:45–52.
39. Ballerstadt R, Gowda A, McNichols R. Fluorescence resonance energy transfer-based near-infrared fluorescence sensor for glucose monitoring. *Diabetes Technol Ther*. 2004;6(2):191–200.
40. Posa A, Brauer L, Schicht M, Garreis F, Beileke S, Paulsen F. Schirmer strip vs. capillary tube method: non-invasive methods of obtaining proteins from tear fluid. *Ann Anat*. 2013;195(2):137–42.
41. Jones DT, Monroy D, Pflugfelder SC. A novel method of tear collection: comparison of glass capillary micropipettes with porous polyester rods. *Cornea*. 1997;16(4):450–8.
42. La Belle JT, Adams A, Lin CE, Engelschall E, Pratt B, Cook CB. Self-monitoring of tear glucose: the development of a tear based glucose sensor as an alternative to self-monitoring of blood glucose. *Chem Commun* (Camb). 2016;52(59):9197–204.
43. Lee SH, Cho YC, Nam DY, Huh BK, Kim SN, Lee DH, Park CG, Choy YB. Designing minimally invasive preocular contact tips for potential application in tear collection. *Cornea*. 2018;37(9):1163–8.
44. Sen DK, Sarin GS. Tear glucose levels in normal people and in diabetic patients. *Br J Ophthalmol*. 1980;64(9):693–5.
45. Potts RO, Tamada JA, Tierney MJ. Glucose monitoring by reverse iontophoresis. *Diabetes Metab Res Rev*. 2002;18(Suppl 1):S49–53.
46. Han JH, Cho YC, Koh WG, Choy YB. Preocular sensor system for concurrent monitoring of glucose levels and dry eye syndrome using tear fluids. *PLoS One*. 2020;15(10):e0239317.
47. Yan Q, Peng B, Su G, Cohan BE, Major TC, Meyerhoff ME. Measurement of tear glucose levels with amperometric glucose biosensor/capillary tube configuration. *Anal Chem*. 2011;83(21):8341–6.
48. Korb DR, Herman JP, Finnemore VM, Exford JM, Blackie CA. An evaluation of the efficacy of fluorescein, rose bengal, lissamine green, and a new dye mixture for ocular surface staining. *Eye Contact Lens*. 2008;34(1):61–4.
49. Asati A, Santra S, Kaittanis C, Nath S, Perez JM. Oxidase-like activity of polymer-coated cerium oxide nanoparticles. *Angew Chem Int Edit*. 2009;48(13):2308–12.
50. Das S, Dowding JM, Klump KE, McGinnis JF, Self W, Seal S. Cerium oxide nanoparticles: applications and prospects in nanomedicine. *Nanomedicine* (Lond). 2013;8(9):1483–508.
51. Garcia-Rey S, Gil-Hernandez E, Basabe-Desmonts L, Benito-Lopez F. Colorimetric Determination of Glucose in Sweat Using an Alginate-Based Biosystem. *Polymers* (Basel). 2023;15(5):1218.
52. Kim JS, Oh HB, Kim AH, Kim JS, Lee ES, Baek JY, Lee KS, Chung SC, Jun JH. A study on detection of glucose concentration using changes in color coordinates. *Bioengineered*. 2017;8(1):99–104.
53. Ornatka M, Sharpe E, Andreescu D, Andreescu S. Paper bioassay based on ceria nanoparticles as colorimetric probes. *Anal Chem*. 2011;83(11):4273–80.
54. Lin Y, Xu C, Ren J, Qu X. Using thermally regenerable cerium oxide nanoparticles in biocomputing to perform label-free, resettable, and colorimetric logic operations. *Angew Chem Int Ed Engl*. 2012;51(50):12579–83.
55. Belmonte C, Acosta MC, Merayo-Llloves J, Gallar J. What causes eye pain? *Curr Ophthalmol Rep*. 2015;3(2):111–21.
56. Lee SH, Cho YC, Bin Choy Y. Noninvasive self-diagnostic device for tear collection and glucose measurement. *Sci Rep*. 2019;9(1):4747.
57. Cai JC, Chen Y, Liu Y, Li S, Sun CH. Capillary imbibition and flow of wetting liquid in irregular capillaries: A 100-year review. *Adv Colloid Interfac*. 2022;304:102654.
58. Mishima S, Gasset A, Klyce SD Jr, Baum JL. Determination of tear volume and tear flow. *Invest Ophthalmol*. 1966;5(3):264–76.
59. Taormina CR, Baca JT, Asher SA, Grabowski JJ, Finegold DN. Analysis of tear glucose concentration with electrospray ionization mass spectrometry. *J Am Soc Mass Spectrom*. 2007;18(2):332–6.

## Publisher's Note

Springer Nature remains neutral with regard to jurisdictional claims in published maps and institutional affiliations.

Ready to submit your research? Choose BMC and benefit from:

- fast, convenient online submission
- thorough peer review by experienced researchers in your field
- rapid publication on acceptance
- support for research data, including large and complex data types
- gold Open Access which fosters wider collaboration and increased citations
- maximum visibility for your research: over 100M website views per year

At BMC, research is always in progress.

Learn more [biomedcentral.com/submissions](https://biomedcentral.com/submissions)

